Fabrication of monophasic strontium-doped calcium silicate granules with enhanced osteogenic performance in the reconstruction of rabbit bone defect

FEI XU[1], EDEM PRINCE GHAMOR-AMEGAVI[2]*, YU CHONG[3]

[1] Department of Orthopedics, The Second People's Hospital of Hefei, Hefei, Anhui 230011, China.

[2] Department of Orthopedic Surgery, the Second Affiliated hospital, School of Medicine of Zhejiang University, Hangzhou 310009, Zhejiang, China.

[3] Department of Orthopedics Affiliated Jiangnan Hospital of Zhejiang Chinese Medical University, Xiaoshan Traditional Hospital Yucai Road-152, Xiaoshan District, Hangzhou, Zhejiang, China.

Purpose: Advances in the design and manufacturing of novel synthetic bioactive scaffolds as bone substitute in bone reconstruction are at the forefront of orthopedic study due to their excellent biological performances. However, fabricating bioactive scaffolds with similar osteogenic and mechanical properties of a natural bone still remains a challenge. Our aim was to produce functional bioactive scaffolds with biologically interactive ions, microstructure for cell proliferation and a suitable biodegradation rate in critical-size bone defect. *Methods*: A homogenous strontium-doped calcium silicate (Sr-CaSi) bioactive granule with interconnected porous network was fabricated. Critical-size bone defect (Ø ~6.5 × 8.5 mm) was created at the distal femur of New Zealand rabbit and the animals were divided into two groups (blank group and implanted/Sr-CaSi group). The blank had no granules while the implanted group was grafted with Sr-CaSi granules at the defect. Bone repair was assed using investigations of micro-CT, 3D argumentation and histological evaluations. *Results*: The Sr-CaSi group had complete bone healing and reconstruction. The granule showed physiochemical tolerance and was able to biodegrade enhancing the formation of new bone matrix and remodeling. However, the blank group had limited proliferation and osteogenic differentiation of new bone tissue, hence there was retarded ingrowth of new bone tissues. *Conclusion*: The Sr-CaSi group saw excellent bone mineralization due to biostimulation effect of the bioceramic granules. The extensive stimulation and osteogenic factors in bone healing by the novel Sr-CaSi shows it is indispensable in bone tissue engineering and regenerative medicine.

Key words: synthetic bioactive scaffolds, bone reconstruction, biostimulation, osteogenic, porous network

1. Introduction

these physiological or pathological deficit bone have great impact on the quality of life of patient that may lead to functional impairment of the affected area. Bone healing is a multicomplex process that involves a lot of mechanism to achieve physiological function. It can be seen in endogenous interaction where there is the deficiency of bone growth endosteal apposition and exogenous condition like physical activity and nutrition compromising the hemeostasis of the bone [13],

[25]. Though it is known that, under natural physiological condition, bone has a high regeneration efficacy, it has a threshold where it cannot anatomically heal by itself, called the critical size defect [2], [28]. By definition, critical size bone defect is size of an osseous defect that does not heal spontaneously during the life time of the animal [14], [36].The complex interplay of bone healing in a critical defect is yet fully not well understood. Hence, there is the need to understand these fracture healing patterns.

The application of bioactive materials in bone tissue regeneration and reconstruction of defects has

---

played an indispensable role in stimulating mesenchymal stem cells and improving bone mineral density. Fabrication technique used in producing bioceramic granules has a significant effect on the bone infiltration and biodegradation of the scaffold. Production of these granules is mostly aided by the use of free dropping or microfluids to form monodisperse beads, which generally involve the use of micro-devices to form NaAlg emulsion droplets with the addition Of Ca^{2+} ions to form $CaCl_2$ solution [9]. The success of these synthetic bone implants depends on angiogenesis, osteointegration and osteogenic factors of the bioceramic material used. Moreover, porous architecture of the scaffolds are crucial for cell infiltration and vascularization. These interconnected pores serve as channel for transport of nutrients with arbitrary similar structural composition closest to that of the natural bone.

Ideally, apart from scaffold bioactive stimulation of the surrounding tissues, they are to provide a 3-dimentional surface structure for the mass transport of nutrients [1]. This helps maintain the biological integrity and characteristic feature of porosity and permeability for functional outcome in new bone growth. Therefore, the use of these bioceramic granules are important to provide neo-vascularization and bone remodeling by integrating well with the surrounding environment to foster osteogenic cellular activities.

Calcium Silicate (CaSi)-based bioceramic materials have received extensive study and have been shown to have noble properties [27], [35]. CaSi has been reported to have positive interaction with biological tissues due to their release of interactive ions like calcium [6], [21] and the nucleation of an apatite layer on their surface [5], [7], [8]. The superiority of CaSi over other fabricated bioactive scaffolds is that the silicate ions derived from it has been shown to reduce inflammatory responses of macrophages and to help promote bone regeneration by inhibiting the activation of NF-ICB signaling pathway [12]. Furthermore, it has been indicated that coatings composed of nanoscale CaSi was able to reduce the rate of degradation of implant, promote cell attachment and their proliferation as well as increase the expression of angiogenic factors [34]. The above-mentioned crucial factors have contributed it use in the clinical setup in bone tissue reconstruction. However, although CaSi has been used in a lot of biomedical studies due to their novel performances, there are some limitations such as (i) high dissolution rate, that is releasing excessive Ca and Si ions which could have negative effect on cell proliferation [19], (ii) have low mechanical stability under physiological loading [18],

and (iii) inadequate osteoconduction and bone growth properties [22].

On the other hand, significant progress has been made in fabricating CaSi composite with specific properties such as micro-structural architecture and physiochemical functions [40]. An example is the incorporation of strontium (Sr) into CaSi bioceramic to form Sr-CaSi composite [37]. This combination phase offers the advantages of both components, with improved osteoid tissue formation and catalysis of bone mineralization. Hereby, we aimed to (i) fabricate porous bioceramic granules with tailored geometric microstructure to scale up osteogenesis and (ii) study the chronological bone healing with and without biomaterial implantation in critical size bone defect. The study analyzed the *in vivo* defect osseous healing interms of new bone growth, remodeling, implant degradation and established local biological effects in skeletally mature New Zealand white rabbits regarding time of using micro-CT (for qualitative and quantitative analysis, 3D) and histological study. Systematic *in vitro* investigation of the homogenous bioceramic granule mechanical property, degree of biodegradation and physicochemical properties were evaluated. This study helped to further understand the behavior of bone healing homeostasis and illustrate how bioactive granules osteosynthesis in the bone defect.

2. Materials and methods

2.1. Powder preparation

Powder was prepared as described in [16], [33]. Here, α-calcium sulfate hemihydrate (αCSH) was made by hydrothermal processing method, where calcium sulfate dehydrate (CSD) powder was treated in 15% NaCl boiling solution and stirred for 5 hours at 100 °C with 0.1% citric acid as morphology modifier [11]. After that, the suspension was filtered and then rinsed 3 times in boiling water and dried at 120 °C for 6 hours. For chemical precipitation, 0.4 $moll^{-1}$ solution of $Ca(NO_3)_2$ with a pH of ~11.4 by stirring. When titration was finished, the solution was stirred for 24 hours, filtered and washed with deionized water and ethanol 3 times, respectively. The dried resultant precipitate was dried for 24 hours at 80 °C and finally calcified at 800 °C for 3 hours. The Sr-CaSi was made by partially replacing the $Ca(NO_3)_2$ with 8% $Sr(No_3)_2$ in molar ration.

2.2. Cement fabrication

The Sr-CaSi was moistened with 0.4 ml/g of de-ionized water and vibrated to form a uniform paste. The paste was then transferred into a mold with internal diameter of ~5.0 mm. At 37 °C, the sample was stored in a water bath with 100% humidity for 2 hours. After hardening, the samples were removed from the mold and dried at room temperature.

2.3. Physiochemical characterization of the powder

The fabricated granules were verified by X-ray diffraction (XRD; Rigaku, Japan) with a CuKα radiation at a scanning rate of 2°/min. Scanning electron microscopy (SEM; JEM-6700F, JEOL) and energy dispersive spectroscopy (EDX) was used to analyze the morphology and microstructure of the granules.

2.4. Evaluation of mechanical property

The compression resistance of the samples ($n = 6$) were measured by universal testing machine (Model4502; Instron, Boston, MA) at the speed of 50 N/min. The maximum compressive strength for crushing the granule was recorded and analyzed.

2.5. Biodissolution *in vitro*

The ion release of the Ca^{2+}/SiO_4^{4-} from the bioceramic granule was studied by immersing the as-sintered microsphere (8 g;Wo) in Tris buffer solution with an initial pH of 7.25 at 37 °C. To stimulate the environment *in vitro*, 2.0 ml of the supernatant was centrifuged at time interval followed by diluting with 5 vol. % HCl solution Si, Ca and Sr ions using inductive couple plasma emission spectroscopy (ICP-AES; Thermo). After every week of immersion, the samples were rinsed with ethanol and then dried at constant mass (W_t) before weighing. The decrease in weigh was expressed as:

$$\text{weight decrease} = W_t/W_0 \times 100\%.$$

At each dilution period, the pH value of the solutions were analyzed by an electrolyte-type pH meter (FE 20K, Metter Toledo, Switzerland).

2.6. Animal bone defect repair

The *in vivo* study followed all animal study protocols and was approved by the Zhejiang University Ethics Committee. A total of 20 New Zealand male rabbits with mean weight of 3.4 kg and average age of 3.5 months were used in this study. The rabbits were randomly divided into two groups (Group A and Group B), with each group consisting of 10 rabbits. Group A (the blank group) had no implantation of bioceramic granules at their bone defect while group B had their bone defects implanted with granules. The distal femoral bone was used for the study. The animals were anesthetized by 3% Sodium phenobarbital dosage of 1 mg/kg for bilateral distal femur defect repair. After sterilization and draping under strict aseptic condition, a ~3 cm longitudinal incision was made on the distal femoral condyle. A dental drill was used to make a bone defect ($\varnothing$ ~6.5 × 8.5 mm) sagittal and longitudinal to the distal femur. Group A ($n = 10$) defect received no granule implantation. The bioceramic granule was implanted in group B ($n = 10$). The incision was then systematically sutured. Post-operatively, the rabbits received Penicillin (80000 U) treatment once a day for 3 days. The rabbits were euthanized at 4, 8 and 12 weeks post-operation for histological and radiological analysis.

2.7. Micro-CT reconstruction analysis

μCT (micro-CT; Inveon^{TM} CT scanner, Siemens, Germany) scanner was used to characterize the animal models and the bone segments with a voltage of 80 kV and current of 80 mA scanning along the axis of the specimen. A pixel size of 14 × 14 cm was used spacing at 14.4 μm to obtain a continuous flat image with a 1024 × 1024 resolution. Using supporting software (IAW, Siemens, Germany) the images were reconstructed to generate coronal, sagittal and 3D color-scale of the regions of interest (ROI, $\varnothing$ 6.0 × 7.5 mm) for morphometric analysis of newly formed bone *in vivo*. Quantitative analysis of trabecular thickness (Tb.Tn), trabecular number (Tb.N), newly formed mineralized bone tissue and residual material (RV/TV) with respect to time, trabecular separation (Tb.Sp) and the ratio of newly formed bone volume versus total volume (BV/TV) were calculated by IAW.

2.8. Histological examination

The harvested specimens were fixed in neutral buffered formaldehyde (8%; pH 7.2) for 2 days and

then rinsed in tap water for 12 hours. The specimen were decalcified for 2 weeks using 10% ethylene ethylenediamine tetra-acetic solution (EDTA) of pH ~7.2. They were then rinsed successively with alcohol solution 80–100% to dehydrate, then washed with toluene and immersed in paraffin, respectively. The extracted specimens were then placed in 4% paraformaldehyde solution for two days. After hardening, they were sliced by saw microtone (SP1600, LEICA, Germany) into sections (100–200 μm in thickness) perpendicular to the longitudinal axis of the bone. The sections were then glued to a plastic support, polished to 4–6 μm thickness and then stained with Van Geison, respectively. Leica microscope was used to measure the histomorphometric parameters and New Bone (NB) was evaluated using Image Pro plus 6.0. The percentage of NB was calculated as:

$$NB\% = \frac{\sum\limits_{n=1}^{5}(\text{newly formed bone area in each photograph/whole area of each photograph})}{5} \times 100\%.$$

2.9. Statistical analysis

Statistical study was done using one-way analysis of variance (ANOVA). Data analysis in this study was expressed as the mean ± standard deviation. A p value of <0.05 was considered as statistically significant.

3. Results

3.1. Phase and morphology of powders

The XRD patterns of the homogenous bioceramic granules are shown in Fig. 1a. The phase composition for the pure αCSH and Sr-CaSi granule were consistent with the as-prepared starting powders.

3.2. SEM observation of the granules

SEM micrograph was used to characterize the micro-architecture and structural morphology of the granules. The polished cross-section of the granule is shown

in Fig. 2b. There were visible open pore at the struts surfaces and moderate densification was also observed at the cross-sectional surface. Moreover, the micrograph indicated hollow and porous structures of the granules that were homogeneously distributed. The average dimension of the granule was ~3.2 × 2.9 × 1.9 mm (length, breath, height respectively).

3.3. Degradation test *in vitro*

ICP analysis was used to study the ion release of the products. The data indicated that the Sr, Ca and Si concentration increased steadily during the 24 days in the immersion media (Fig. 3a–c). As for the change in pH value after immersion in Tris buffer, there was an overall rise (Fig. 3d) during the whole immersion stage. The pH on the second day of immersion was 7.72, then slightly rose to 8.2 on day 6 due to dissolution of the residual granules and then reached a maximum peak of 8.89 on day 12 after soaking. The biodegradation behavior of the Sr-CaSi granules in Tris buffer solution is shown in Fig. 3e. The bioceramic granule showed a modest fast biodissolution throughout the whole immersion stage (7 Weeks). The Sr-CaSi granule underwent a weight decrease of 23.14% for the first 2 weeks in Tris buffer solution. This can be attributed to the dissolution of the surface construct when in contact with the solution. Further immersion of the granule showed a faster weight decrease comparatively from week 3 to week 5, losing a total of 59.27% which represents over half of its original weight. Due to continuous dissolution and degradation of the granule. From week 6 to the final immersion week 7, the granule had 8.95% of the residual left in the medium. The slightly lower biodegradation at the end of the study could be caused by the recrystallization of the bioceramic granule with the solution medium and granule surface.

The results of the maximum compressive load in crushing the sample is shown in Fig. 3f. It was found that the Sr-CaSi crushing load was approximately 9.2 N.

3.4. Primary evaluation and micro-CT analysis of the animal models

The animal study was done under standard conditions. The bone defects in both the blank group and the group with implanted granules saw no local infection and inflammation at the site. During post-surgery
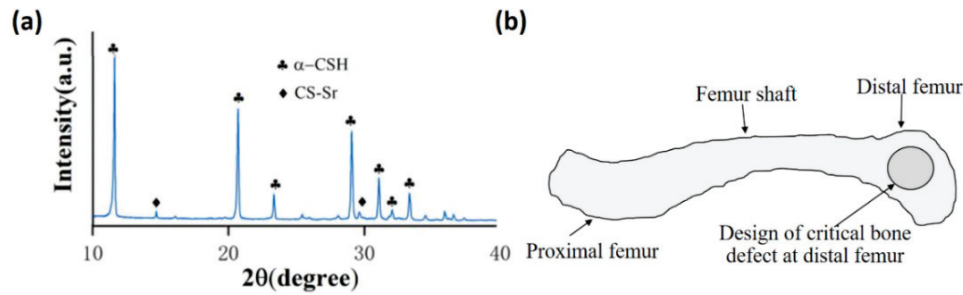
Fig. 1. (a) XRD patterns of the as-dried bioceramic granules Sr-CaSi,
(b) femoral bone of a rabbit; distal critical-size bone defect area ($\varnothing$ ~6.5 × 8.5 mm)
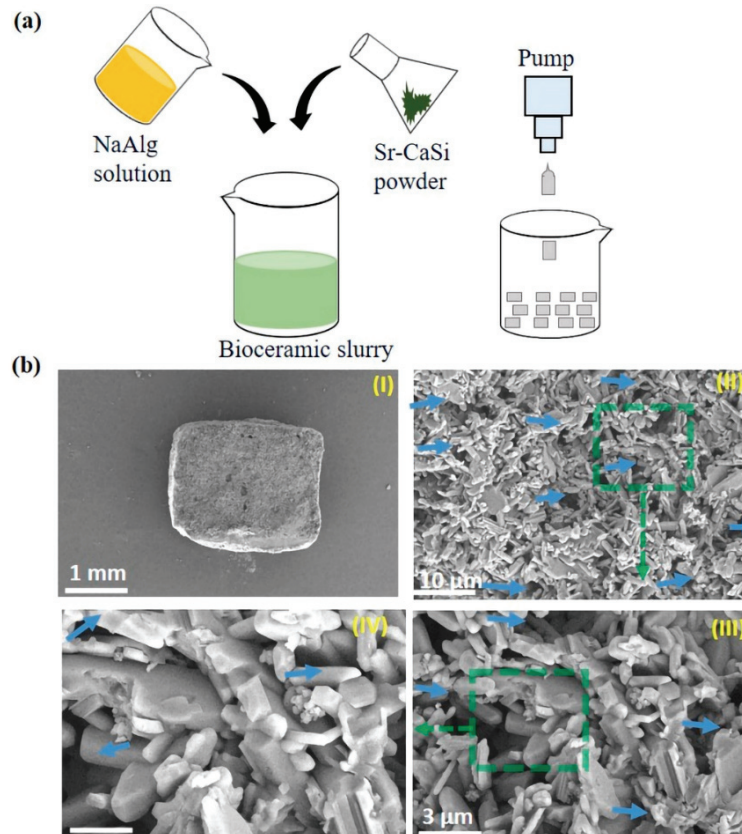

Fig. 2. (a) schematic illustration of the preparation of the granule slurry,
(b) SEM micrographs of the granules, blue arrows showing the micropores

clinical evaluation, the animals were healthy, their eating habits were normal and did not record any weight loss. The harvested samples showed visible healing of the bone defect for the implanted group while the group without any implanted granules saw partially healed defect (Fig. 4). 3D micro-CT reconstruction (Fig. 5) displayed a systematical biodegradation and bioresorption of the granule from week 4 to week 12.

3.5. µCT reconstruction analysis

The reconstructed images of both groups displaced similar pattern of new bone growth from the edges of the defect to the center at the first 4 weeks. The Sr-CaSi grafted defects displayed the most abundance of newly formed osteoid tissues compared to the non-grafted group. However, the non-grafted group showed reasonable new bone ingrowth but not enough to fully heal the defect. At week 4, the bone repair in the non-implanted group was similar to that of the Sr-CaSi group exhibiting interconnected bone macropore structures. With the continuation of time (week 8), there was an increase in new woven bone growth with remolding of the defect. However, the control group showed minor amount of new bone accumulation. At week 12, regeneration in control group was seen to have decreased and the closure of the defect was still not complete. Com-
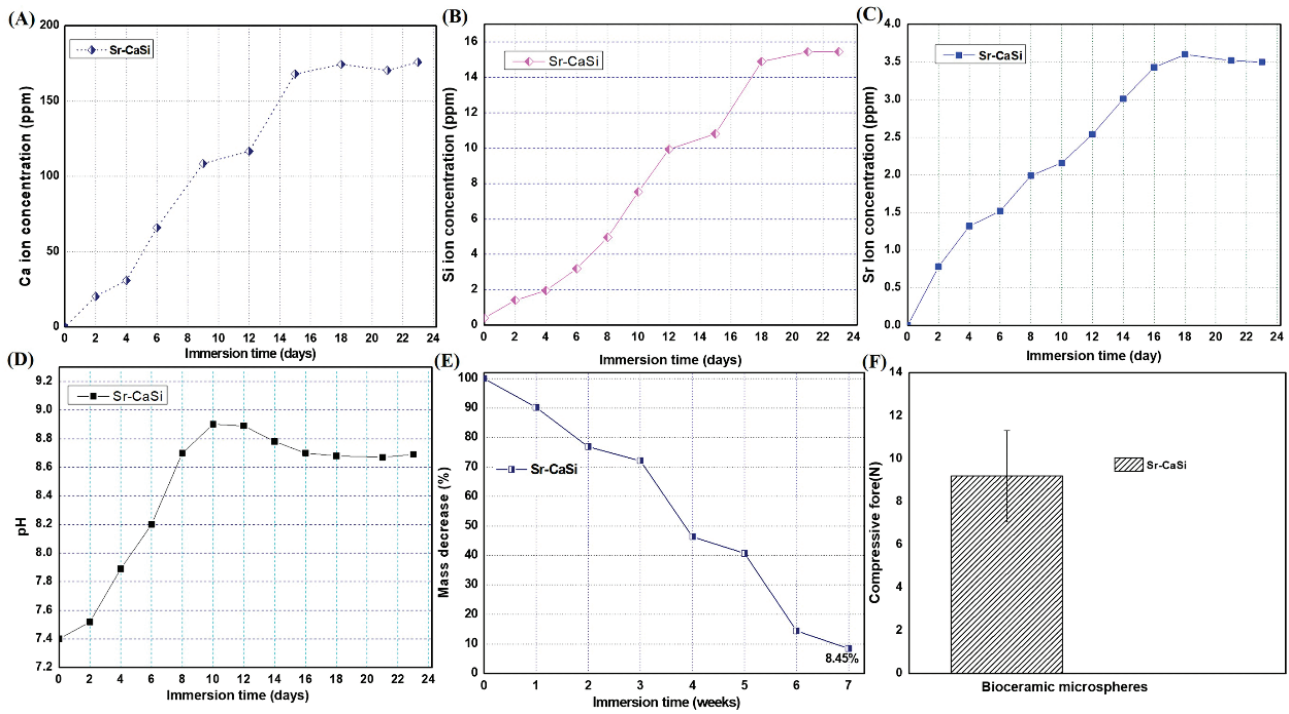
Fig. 3. (A)–(C) *in vitro* biodisolution test for the bioceramic granules in Tris buffer solution, (D) changes in pH values within 24 days, (E) Mass loss during 7 weeks of immersion, (F) Compressive force for crushing the granule

paring of the results obtained at the different experimental time line indicated that the group implanted with Sr-CaSi scaffold increased steadily with new bone density and was able to achieve advanced bone reconstruction and total healing of the defect.

On the other hand, comparing the Sr-CaSi group at week 4 and 8 saw visible active fragmentation and dissolution of the scaffold composite. By the end of the 12th week of the study, the biomaterial had degraded leaving just a little behind. The results were consistent with quantitative μCT segmental analysis (Fig. 6). The Sr-CaSi group and the control group both showed high bone volume and trabecular, representing new bone growth at the defect for the first 4 weeks. There was no significant difference in BV/TV and Tb.N in these two groups. However, from week 8 to week 12, the Sr-CaSi group showed significantly high BV/TV and Tb.N. The Sr-CaSi residual volume during the 4–12 weeks reduced dramatically due to biodecay of its material giving more room for new bone matter infiltration.
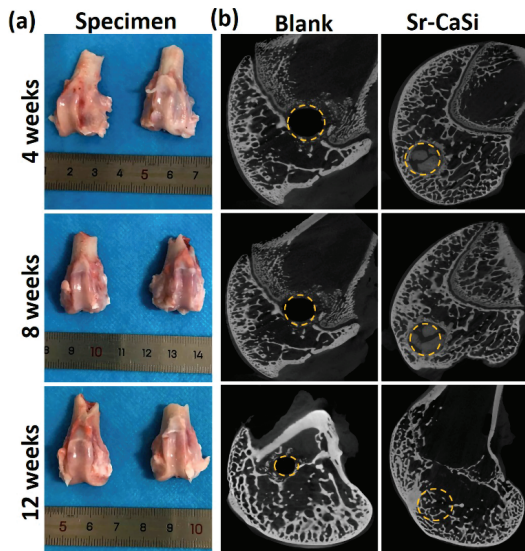

Fig. 4. Primary evaluation and radiographic analysis of the bone specimens: (a) harvested bone samples, (b) μCT images femoral bone specimens indicating the position of the defect (yellow markings)
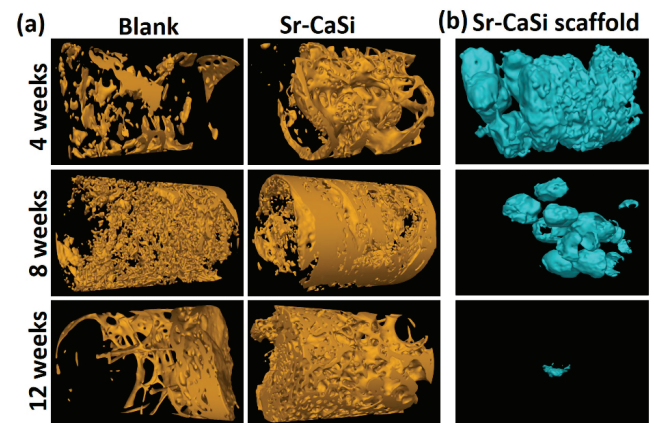

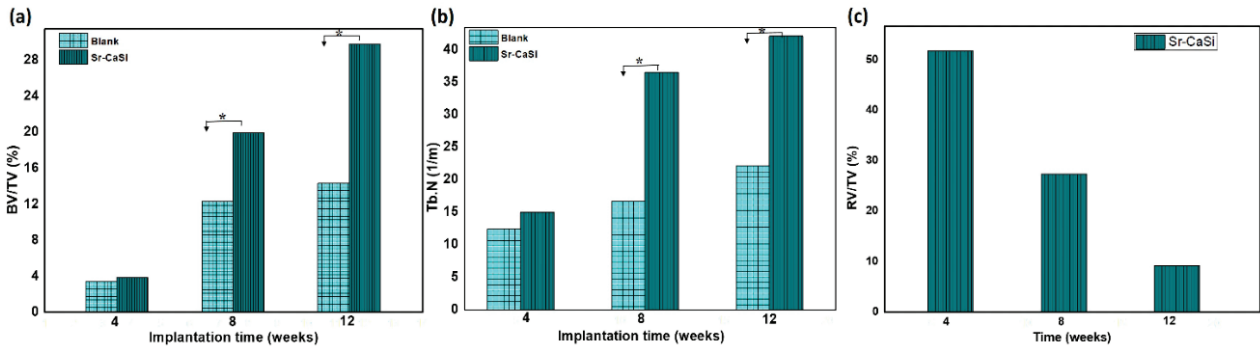Fig. 5. 3D μCT reconstruction of new bone: (a) newly formed bone matrix, (b) material biodegradation with time

Fig. 6. μCT quantitative analysis BV/TV (a) and Tb.N f (b) for the animal models; * $p < 0.05$

3.6. Histological analysis

The histological sections of the specimen stained with HE is displayed in Fig. 7. None of inflammatory cells or fibrous connective tissues at the defect were observed. Histology confirmed osteoblastic activity and infiltration of new bone tissues at the defect site. Periosteal ridge of newly formed osteoid covered the defect surface in both groups. For the Sr-CaSi group, there was colonization and biodegradation of the biomaterial which started at the surface and then penetrated through the porous construct. At magnification, it was possible to observe the neoformed bone with biodegraded granules. The granule hematopoietic bone marrow could also be seen at the implant site. H.E imaging indicated new bone (NB) in both Sr-CaSi and the blank group was similar with both having colonies of newly formed osteoid tissues visible at the defect at week 4. From week 8 to week 12 the region of newly formed bone increased indicating osteogenesis in both groups. However, the group treated with Sr-CaSi graft showed superior osteoid organization and mineralization during the defect healing and reconstruction. Moreover, apart from rich vascularized connective tissues with blood vessels and matured trabecular which occupied the defect, there was also replacement of the biomaterial with new bone visible at week 12. There was significant formation of lamellar bone tissues concentrated with osteoid activity and vascularized connective tissues especially at the Sr-CaSi site.
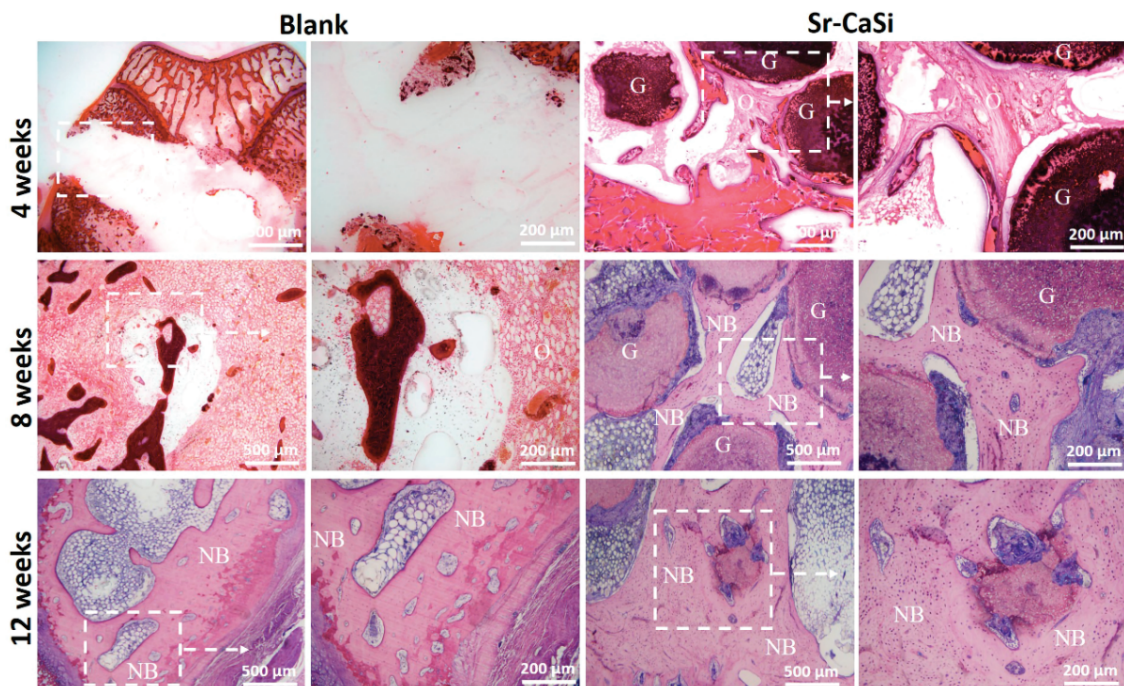

Fig. 7. HE staining and histological observation of new bone regeneration in both bone defects.
NB – new bone, G – granule

4. Discussion

Orthopedic fractures and bone defects may occur due to a variety of reasons like trauma, infection and pathological conditions. With a deficit in bone structure, alternative method, such as tissue engineering and regenerative medicine, are needed for bone healing and reconstruction. It has been noted that new bone formation is stimulated by the activation of mesenchymal stem cells and their absorption onto surfaces with nanoscale topographic features [15]. The activity and number of these stem cells play a crucial role in bone defect repair [26] and, therefore, when these factors are affected, lead to delay in bone healing and cause nonunion [24], [39]. "Healers" or grafts with unique inherent biological advantage such as biocompactibility, being physiologically friendly to the surround tissues and having osteogenic effect for bone healing. In big defects reconstruction, synthetic bone grafts or biomaterials are needed not only to fill the void, but also to stimulate new bone formation to restore original condition.

The aim of this study was to investigate the healing process of critical-size distal femoral defect under natural healing condition and treatment with bioactive Sr-CaSi granules. For this purpose we fabricated a homogenous Sr-CaSi scaffold with tailored physiochemical property and biological performance. We analyzed (i) the histological and micro-CT (qualitative and quantitative) outcome of both defects with and without Sr-CaSi graft and (ii) osteogenic cell adhesion, proliferation and extracellular stimulation capacity of the fabricated granule. In this regard, the bone regeneration was evaluated from 4 to 12 weeks. The data collected in this study confirmed that the defect with grafted Sr-CaSi saw more beneficial results with high presence of new bone formation, which could be attributed to osteostimulation by the bioactive ions that help improve tissue metabolism at the implanted site

and also enhanced microcirculation of nutrients. This leads to the entire volume of defect being healed. Hence, it is reasonable to say that porous bioceramic granules accelerated the normal osteogenesis of the bone healing.

It has been documented that research is prone to influencing the physiochemical and biological properties of biomaterials [3], [29], [38] to improve the integrity and functional outcome in the body. In this study, Sr was incorporated into CaSi to facilitate the transport of atoms and also encourage the stimulating phase of CaSi transition [20]. We succeeded in fabricating homogenous granule with unique osteogenic angiogenesis ability to investigate bone reconstruction efficacy in critical size bone defect. 3D visualization showed that the Sr-CaSi group had superior new bone geometrical structures in the defect at the end of the study this and was consistent with quantitative BV/TV and Tb.N analysis. On the other hand, the blank group defect was partially filled with new bone ingrowth. This implies that the bone volume callus for the Sr-CaSi group was significantly higher than the blank group and was able to fully heal the defect. Comparative study using H.E staining confirmed the micro-CT analysis indicating that the Sr-CaSi had more enhanced new bone formation with increase in bone density compared to the blank group. The significantly high bone formation in the Sr-CaSi group at week 12 could be explained as a result of precipitation action of its surface providing osteogenic cell support at the site of defect. The other reason why Sr-CaSi group had exponential new bone ingrowth could be it being able to promote fibroblast aggregation increasing osteoblast deposition which plays a crucial role in bone mineralization.

Proposed reaction of the Sr-CaSi in physiological environment is illustrated in Fig. 8. In the first or early stage, there is the hydration and exchange of ions with the scaffold and surrounding physiological fluid. The resultant hydration (OH^-) in the surrounding tissues boast an increase in the pH level. This increase in pH
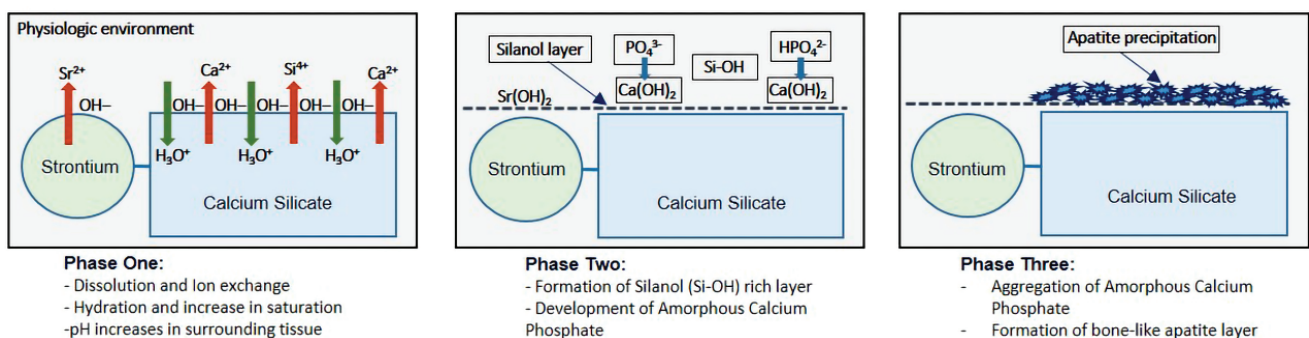

Fig. 8. Schematic illustration of the different phases of apatite forming systems in a physiological environment
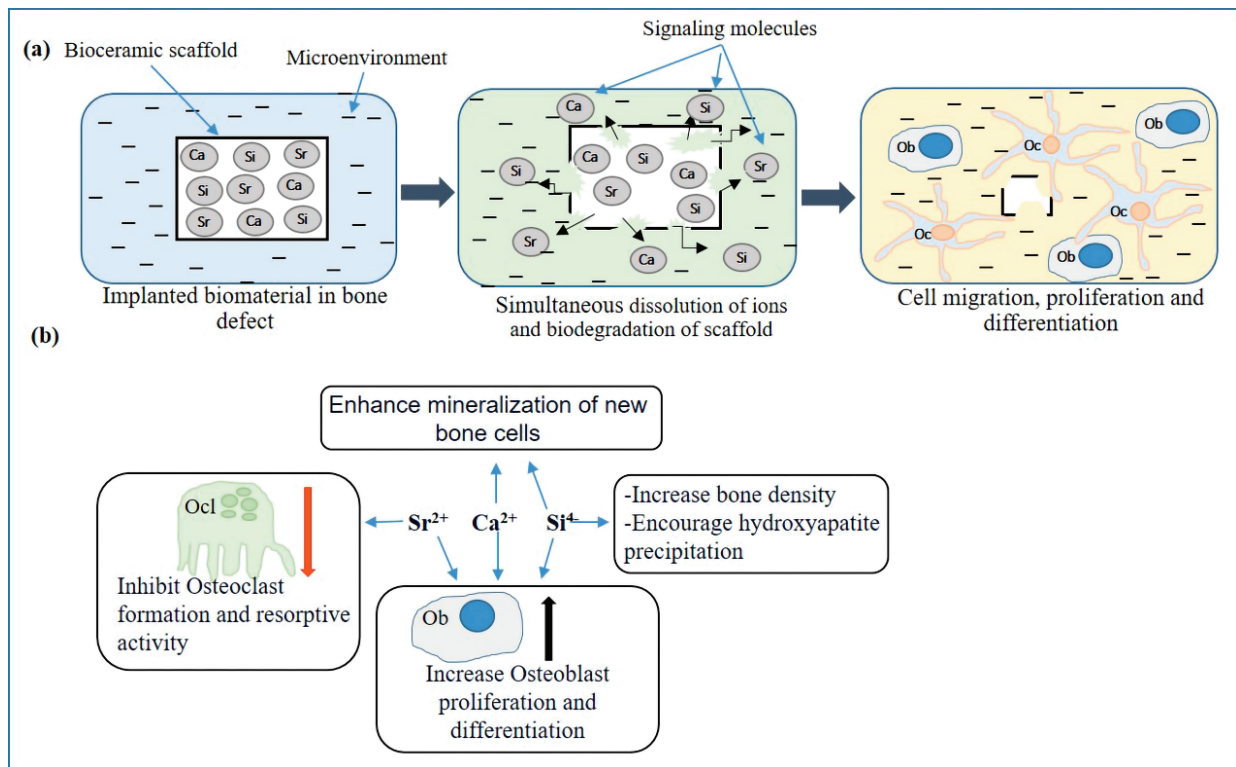
Fig. 9. Mechanism of biomaterial dissolution and trigger of osteogenesis, (d) indicate role ions play in bone tissue formation.
Ob – osteoblast, Oc – ostecyte, and Ocl – osteoclast

makes the area alkaline and help trigger and promote tissue repair [4], [30]. On the second stage, there is the reaction of Ca^{2+} with OH^- to form amorphous calcium hydroxide $(Ca(OH^-)_2)$ and also simultaneous formation of silanol (Si-OH) rich layer on the surface of the bioceramic granule. The silanol forms the main binding phase [23]. In the final stage, there is the aggregation of the amorphous calcium hydroxide which leads to the formation of a bone-like apatite layer on the surface of the substrate. On the other hand, the dissolution and biodegradation of the granule triggers osteoid cells for new bone growth, as illustrated in Fig. 9.

The recruitment of mesenchymal cells, proliferation, differentiation and release of extracellular matrix is known to be important for tissue formation [31], [32]. Li et al. [17] in their study demonstrated high activity of Sr ions on osteoblast cells and were effective in improving cellular attachment and subsequent cell activities for bone regeneration. At the first 4 weeks post-operation, general histological findings indicated that the specimen in both groups had similar good healing but had difference in the degree of new bone ingrowth. Comparing the blank group with the Sr-CaSi group at week 8, a wider region of bone tissue formation was observed in the bioceramic group. This finding indicated that early stage of osteoid formation was initiated among the connective tissues. It is important to note that the increased bone volume in the Sr-CaSi group was a result of the continuous angiogenesis and remodeling of bone marrow stem cells by the biomaterial. Gu et al. [10] reported that bone marrow microenvironment consists of heterogeneous mix of hematopoietic and non-hematopoietic cells which provide crucial cues that regulate new bone formation at local and systemic levels. In our study, histology revealed extensive regions of new bone growth occupied by interwoven bone trabeculae with substantial deposition of osteoblast for the Sr-CaSi group at week 12. This result indicated that the Sr-CaSi had high biological affinity to the surrounding bone defect. *In vitro* test during immersion of the granules in Tris buffer solution provided a more insight on the biodissolution and biodegradation of the bioceramic granules. It was evident that the Sr-CaSi underwent leaching of Si, Ca and Sr ions from the porous construct. These tailored biodissolution from the scaffold is beneficial to stimulate osteogenesis. The limitation in this study was the fabrication of a bioactive scaffold with porous architecture that has the same osteogenic and mechanical properties of a natural bone. On the other hand, further studies are needed to investigate the effects of ionic dissolution of bioceramic granules in osteogenic stem cell activity during new bone regeneration.

5. Conclusion

Our study successfully fabricated excellent biocompactible material that served as an osteogenic catalyst which was sufficient to promote full healing and reconstruction in a critical-size bone defect. The blank group showed different degree of bone healing in comparism with the Sr-CaSi group. Sr-CaSi group exhibited radiographical and histological effects interms of new bone growth and reconstruction of the defect. From data analysis, the blank group does not have consistent effect on bone regeneration by itself. *In vivo* implantation of the Sr-CaSi showed that the rate of newly formed bone was faster and further histological analysis indicated more proliferation and differentiation of new bone cells than the blank group. The study demonstrate that Sr-CaSi has good bonding with the surround microenvironment. This excellent biocompactibility contributed to rapid new bone regeneration with higher quality bone mass. Therefore, it is crucial to fabricate biologically stable bioactive granules with improved physiochemical property and inherent ability for repair and reconstruction of bone defect.

Authors information

Fei Xu: Preparation of the research program, execution of research and preparation of manuscript. Ghamor-Amegavi Edem Prince: Preparation of research program, statistical analysis, interpretation of data and obtaining financing. Yu Chong: Interpretation of data and preparation of manuscript.

Acknowledgements

Conflict of interest

All authors have no conflict of interest.

Ethical approval

This study was approved by the Zhejiang University Ethics Committee.

References

[1] ARSLAM-YILDIZ A., ASSAL R.E., CHEN P., INCI F., DEMIRCI U., *Towards artificial tissue models: past, present, and future of 3D bioprinting*, Biofabrication, 2016, 8, 014103.

[2] CACCHIOLI A., SPAGGIARI B., RAVANETTI F., MARTINI F.M., BORGHETTI P., GABBI C., *The critical sized bone defect: morphological study of bone healing*, Ann. Fac. Med. Vet. di Parma, 2006, XXVI, 97–110.

[3] ELFEKI H., FIALLO M., SHARROCK P., MBARKI M., *Hydroxyapatite bioceramic with large porosity*, Mater Sci. Eng. C, 2017, 76, 985–990.

[4] FERRACANE J.L., COOPER P.R., SMITH A.J., *Can interaction of materials with the dentin-pulp complex contribute to dentin regeneration?*, Odontology, 2010, Vol. 98, 1, 2–14.

[5] GANDOLFI M.G., CIAPETTI G., TADDEI P., PERUT F., TINTI A., CARDOSO M.V., MEERBEEK B., PRATI C., *Apatite formation on bioactive calcium-silicate cements for dentistry affects surface topography and human marrow stromal cells proliferation*, Dent. Mater, 2010, 26, 974–992.

[6] GANDOLFI M.G., SIBONI F., BOTERO T., BOSSÙ M., RICCITIELLO F., PRATI C., *Calcium silicate and calcium hydroxide materials for pulp capping: Biointeractivity, porosity, solubility and bioactivity of current formulations*, J. Appl. Biomater. Funct. Mater, 2015, 13, 43–60.

[7] GANDOLFI M.G., TADDEI P., MODENA E., SIBONI F., PRATI C., *Biointeractivity-related versus chemi/physisorption-related apatite precursor-forming ability of current root end filling materials*, J. Biomed. Mater Res., 2013, 101, 1107–1123.

[8] GANDOLFI M.G,, VAN LANDUYT K., TADDEI P., MODENA E., VAN MEERBEEK B., PRATI C., *Environmental Scanning Electron Microscopy Connected with Energy Dispersive X-ray Analysis and Raman Techniques to Study ProRoot Mineral Trioxide Aggregate and Calcium Silicate Cements in Wet Conditions and in Real Time*, J. Endod., 2010, 36, 851–857.

[9] GHAMOR-AMEGAVI E.P., YANG X.Y., FU J., PAN Z.J., ZHUANG C., KE X.R., ZHANG L., XIE L.J., GAO C.Y., GOU Z.R., *Yolk-porous shell biphasic bioceramic granules enhancing bone regeneration and repair beyond homogenous hybrid*, Materials Science & Engineering C, 2019, 100, 433–444.

[10] GU Z., WANG H., LI L., WANG Q., YU X., *Cell-mediated degradation of strontium-doped calcium polyphosphate scaffold for bone tissue engineering*, Biomed. Mater, 2012, 7, 065007.

[11] HINA A., NANCOLLAS G.H., *Alpha calcium sulfate hemihydrate and a method of making alpha calcium sulfate hemihydrate*, International Patent, 2001, WO 0179116.

[12] HUANG Y., WU C., ZHANG X., CHANG J., DAI K., *Regulation of immune response by bioactive ions released from silicate bioceramics for bone regeneration*, Acta Biomater., 2018, 66, 81–92.

[13] HUH S.Y., GORDON C.M., *Vitamin d deficiency in children and adolescents: epidemiology, impact and treatment*, Endocr. Metab. Disord., 2008, 9, 161–170.

[14] JASTY M., BRAGDON C.R., SCHUTZER S., RUBASH H., HAIRE T., HARRIS W.H., *Bone ingrowth into porous coated canine total hip replacements. Quantification by backscattered scanning electron microscopy and image analysis*, Scanning Microsc., 1989, 3, 1051–1057.

[15] JONES J.R., *New trends in bioactive scaffolds: The importance of nanostructure*, J. Eur. Ceram. Soc., 2009, 29, 1275–1281.

[16] LIN K., CHANG J., ZENG Y., QIAN W.J., *Preparation of macroporous calcium silicate ceramics*, Mater Lett., 2004, 58, 2109–2113.

[17] LI Q., WU Y., KANG N., *Marrow adipose tissue: its origin, function, and regulation in bone remodeling and regeneration*, Stem. Cells Int., 2018, 2018, 7098456.

[18] LIU Z.H., HE X.Y., CHEN S.P., YU H.M., *Advances in the use of calcium silicate-based materials in bone tissue engineering*, Ceramics International, 2023, 49, 19355–19363.

[19] MENG W., ZHANG W.X., ZHANG X., NASIRI-TABRIZI B., LI Q., *Doping effects of Pd2$^+$ on physicochemical and biomechanical properties of calcium silicate in nano-regime towards treating osteoporotic bone*, Mater Chem. Phys., 2021, 267, 124609.

[20] MESTRES G., LE VAN C., GINEBRA M.P., *Silicon-stabilized α-tricalcium phosphate and its use in a calcium phosphate cement: characterization and cell response*, Acta Biomater., 2012, 8, 1169–1179.

[21] MIZUNO M., BANZAI Y., *Calcium ion release from calcium hydroxide stimulated fibronectin gene expression in dental pulp cells and the differentiation of dental pulp cells to mineralized tissue forming cells by fibronectin*, Int. Endod. J., 2008, 41, 933–988.

[22] NI S., CHANG J., CHOU L., *A novel bioactive porous CaSiO$_3$ scaffold for bone tissue engineering*, J. Biomed. Mater Res. Part A, 2006, 76, 196–205.

[23] NIU L.N., JIAO K., WANG T.D., ZHANG W., CAMILLERI J., BERGERON B.E., FENG H.L., MAO J., CHEN J.H., PASHLEY D.H., TAY F.R., *A review of the bioactivity of hydraulic calcium silicate cements*, Journal of Dentistry, 2014, 42 (5), 517–533.

[24] ONO N., KRONENBERG H.M., *Bone repair and stem cells*, Curr. Opin. Genet. Dev., 2016, 40, 103–107.

[25] PARFITT A.M., *The two faces of growth: benefits and risks to bone integrity*, Osteoporosis Int., 1994, 4, 382–398.

[26] PEREZ J.R., KOUROUPIS D., LI D.J., BEST T.M., KAPLAN L., CORREA D., *Tissue engineering and cell-based therapies for fractures and bone defects*, Front. Bioeng. Biotechnol., 2018, 6.

[27] RUAN Z., YAO D., XU Q., LIU L., TIAN Z., ZHU Y., *Effects of mesoporous bioglass on physicochemical and biological properties of calcium sulfate bone cements*, Appl. Mater Today, 2017, 9, 612–621.

[28] SCHEMITSCH E.H., *Size matters: defining critical in bone defect size!*, J. Orthop Trauma, 2017, 31, S20–S22.

[29] SHAO H., KE X., LIU A., SUN M., HE Y., YANG X., FU J., LIU Y., ZHANG L., YANG G., *Bone regeneration in 3D printing bioactive ceramic scaffolds with improved tissue/material interface pore architecture in thin-wall bone defect*, Biofabrication, 2017, 9, 025003.

[30] SIQUEIRA J.F., LOPES H.P., *Mechanisms of antimicrobial activity of calcium hydroxide: a critical review*, International Endodontic Journal, 1999, Vol. 32, 5, 361–369.

[31] SUZUKI T., MIYAMOTO T., FUJITA N., NINOMIYA K., IWASAKI R., TOYAMA Y., *Osteoblast-specific Angiopoietin 1 overexpression increases bone mass*, Biochem. Biophys. Res. Commun., 2007, 362 (4), 1019e1025.

[32] TAMBURSTUEN M.V., RESELAND J.E., SPAHR A., BROOKES S.J., KVALHEIM G., SLABY I., *Ameloblastin expression and putative autoregulation in mesenchymal cells suggest a role in early bone formation and repair*, Bone, 2011, 48 (2), 406e413.

[33] WANG J.C., ZHANG L., SUN X.L., CHEN X.Y., XIE K.L., LIN M.A., YANG G.J., XU S.Z., XIA W., GOU Z.R., *Preparation and in vitro evaluation of strontium-doped calcium silicate/gypsum bioactive bone cement*, Biomed. Mater, 2014, 9, 045002.

[34] WANG X., ZHOU Y., XIA L., ZHAO C., CHEN L.D., CHANG J., HUANG L., ZHENG X., ZHU H., *Fabrication of nano-structured calcium silicate coatings with enhanced stability, bioactivity and osteogenic and angiogenic activity*, Colloids Surf. B Biointerfaces, 2015, 126, 358–366.

[35] WEI C.K., DING S.J., *Acid-resistant calcium silicate-based composite implants with high-strength as load-bearing bone graft substitutes and fracture fixation devices*, J. Mech. Behav. Biomed. Mater, 2016, 62, 366–383.

[36] WIERZCHOŚ J., FALCIONI T., KICIAK A., WOLIŃSKI J., KOCZOROWSKI R., CHOMICKI P., POREMBSKA M., ASCASO C., *Advances in the ultrastructural study of the implant-bone interface by backscattered electron imaging*. Micron. Int. Res. Rev. J. Microsc., 2008, 39, 1363–1370.

[37] WU C., RAMASWAMY Y., KWIK D., ZREIQAT H., *The effect of strontium incorporation into CaSiO$_3$ ceramics on their physical and biological properties*, Biomaterials, 2007, 28, 3171–3181.

[38] XIE Y., RUSTOM L.E., MCDERMOTT A.M., BOERCKEL J.D., JOHNSON A.J.W., ALLEYNE A.G., HOELZLE D.J., *Net shape fabrication of calcium phosphate scaffolds with multiple material domains*, Biofabrication, 2016, 8, 015005.

[39] ZAIDI N., NIXON A.J., *Stem cell therapy in bone repair and regeneration, in Skeletal Biology and Medicine*, Pt B: Disease Mechanisms and Therapeutic Challenges, 2007, 62–72.

[40] LIU Z.H., HE X.Y., CHEN S.P., YU H.M., *Advances in the use of calcium silicate-based materials in bone tissue engineering*, Ceramics International, 2023, 49, 19355–19363.